



Full Text View

[Volume 28, Issue 6 \(June 1998\)](#)

Journal of Physical Oceanography

Article: pp. 1271–1286 | [Abstract](#) | [PDF \(376K\)](#)

Order and Resolution for Computational Ocean Dynamics

Brian G. Sanderson

School of Mathematics, UNSW, Sydney, Australia

(Manuscript received September 23, 1996, in final form September 30, 1997)

DOI: 10.1175/1520-0485(1998)028<1271:OARFCO>2.0.CO;2

ABSTRACT

An ocean flow that has all its scales resolved on a model grid can be more efficiently calculated to within a required accuracy by using high-order numerics than by grid refinement with low-order numerics. The differencing order must be at least as great as the space–time dimensionality D of the model to ensure that grid refinement reduces truncation error at least as quickly as computational cost increases. Ocean flows often have variability on a wide range of scales that cannot all be resolved on any practical grid. In such circumstances the distribution of variability among the scales determines whether grid refinement or increased order results in the greatest accuracy per unit computational cost. A model that simulates the $-5/3$ power law of the inertial subrange of three-dimensional turbulence would most efficiently exploit low-order numerics for all terms. The spectra of different terms in the equations of motion can be different and can therefore require different orders of accuracy for efficient computation. Modeling geophysical turbulence with a power law of -3 would require high-order numerics for the advective terms but low-order numerics would be sufficient for other terms. Output from several ocean models are observed to have spectra that are sufficiently red to justify using high-order numerics for all terms. In the case of one relatively simple ocean modeling problem the author demonstrates that leading-order terms dominate the truncation error.

1. Introduction

Most ocean models use either first- or second-order numerics ([Haidvogel and Beckmann 1997](#)). Recently, there has been some interest in applying high-order numerical schemes to ocean models. Some terms are computed to fourth-order accuracy in the DieCAST model ([Dietrich et al. 1990](#))—although time stepping is formally first-order and the elliptic pressure equation is second-order. The usual rationale for mixed-order numerics is that different parts of the calculation affect the ultimate solution to different extents, so more important dynamical terms should be calculated more accurately

Table of Contents:

- [Introduction](#)
- [Order, resolution, accuracy,](#)
- [Field singularities and](#)
- [Truncation error and](#)
- [The applicability of](#)
- [Conclusions](#)
- [REFERENCES](#)
- [TABLES](#)
- [FIGURES](#)

Options:

- [Create Reference](#)
- [Email this Article](#)
- [Add to MyArchive](#)
- [Search AMS Glossary](#)

Search CrossRef for:

- [Articles Citing This Article](#)

Search Google Scholar for:

- [Brian G. Sanderson](#)

than lesser terms. [Mahaevan et al. \(1996\)](#) and [Bender \(1996\)](#) both favor third-order advection schemes over lower-order schemes. [McCalpin \(1994\)](#) uses a fourth-order approximation of horizontal gradients to improve the performance of σ -coordinate models. [Iskandarani et al. \(1994\)](#) and [Haidvogel et al. \(1997\)](#) also explore the use of higher-order methods.

The order of accuracy of numerical calculations would seem to be a fundamental property of any ocean model that critically effects model performance and effective application of the model to obtain solutions to problems in physical oceanography. In order to improve accuracy of numerical solutions we can reduce the grid scale or increase the order of accuracy of numerical operators. The following work evaluates the relative advantage of these two strategies in the context of modeling ocean dynamics.

The advantages of high-order numerics have been demonstrated for numerical weather prediction ([Purser and Leslie 1988](#); [Leslie and Purser 1992](#)). Similarly, [Leonard et al. \(1996\)](#) find that high-order numerics are advantageous for advective problems that they tested. This manuscript will demonstrate why the high-order numerical schemes tested above resulted in superior efficiency relative to low-order schemes and why high-order numerics are not advantageous in all circumstances.

Parenthetically, it should be observed that two different numerical schemes of the same order can have different magnitude truncation errors and grossly different computational costs. This important point is not addressed by the present manuscript. Nevertheless, the results and methodologies of the present manuscript are broadly applicable and can be customized for a wide range of numerical schemes. In this sense, the work presented below is a fundamental design criteria for ocean models when addressing questions of accuracy and computational efficiency.

Fluid flow is generally four-dimensional: three space dimensions and time. Fluid motion is often highly nonlinear and analytically intractable. Sometimes problems of reduced dimensionality occur in the ocean. Tides, for example, might be considered essentially two-dimensional in space plus the time dimension. Indeed, many large and mesoscale oceanic phenomena have slowly varying and largely horizontal motion even though the models often used to study them are four-dimensional. In the case of sufficiently smooth flows then, leading terms dominate the error of the numerical truncation. [Section 2](#) shows that grid refinement, numerical order of accuracy, and the model's dimensionality are not independent quantities for the efficient computation of accurate solutions to such smooth flows.

The ocean has variability over a range of scales vastly greater than can be resolved using computers that are presently available. In [section 3](#) the issue of gradients in ocean properties is addressed and this raises a significant doubt as to the applicability of an asymptotic limit at which the flow can be considered sufficiently smooth. There will always be some part of the flow that can only be modeled by increasing resolution (whereas increasing the order of differencing can only reduce truncation errors on scales already resolved). At a given grid scale flow features with wavenumbers greater than some cutoff wavenumber k_c might be regarded as being unresolved, whereas those with wavenumbers less than k_c could be considered as being resolved. We might, therefore, regard the error as consisting of two parts, the first due to unresolved flows and the second due to truncation errors from differencing resolved flows. In [section 4](#) we present an analysis that demonstrates how the relative importance of these two sources of error is a function of the spectral properties of the flow being modeled and how this determines the advantage of grid refinement relative to increasing the differencing order.

The fields from several different models of ocean flows are analyzed in [section 5](#) in order to determine if these models might better calculate the flows that they model by increasing the numerical order of differencing or by increasing the grid resolution. The relative magnitudes of the first few terms in the truncation series are also computed directly for an idealized two-gyre ocean modeled using a numerical scheme that has high-order spatial differencing.

2. Order, resolution, accuracy, and computational cost

Consider an ocean flow that is to be calculated using numerical differencing techniques on a grid of scale Δ . Let us, for the moment, assume that the flow is sufficiently smooth so that all its scales of variability are resolved at the chosen grid scale. The error ϵ of a numerical solution is proportional to grid scale Δ raised to the power of the order of accuracy m of some numerical method that might be used to solve PDEs and boundary conditions that describe the ocean. This result is expressed as

$$\epsilon = a\Delta^m, (1)$$

where a is a proportionality constant that is a function of the numerical scheme and the differential properties of the problem being solved. [Equation \(1\)](#) is only applicable when the error is dominated by the leading term in the error expansion. As long as the flow is differentiable, then the leading term will always dominate the error if Δ is made sufficiently small.

The goal of numerically modeling the ocean is to closely approach the solution for the corresponding continuum equations. It follows that issues of model design should focus on the behavior of numerical models at grid resolutions where the above goal might be achieved. All of the following work will consider grid scales sufficiently small so that it can be taken

as a given that

$$\frac{\epsilon}{a} < 1$$

since otherwise one could have little faith that the numerical calculation would give results consistent with the solution to the corresponding continuum equations.

The computational cost C of a numerical calculation often increases approximately proportional to the order of accuracy m of the numerical operator and also proportional to the number of points (in space and time) that are operated on. For a given model domain, the number of model grid points is proportional to the inverse of grid scale Δ raised to the power of the model dimension D , so

$$C = bm\Delta^{-D}, (2)$$

where b is a proportionality constant that can be estimated from the number and type of computational operations in a numerical scheme. Thus, different families of numerical schemes will have different values for b . Computational cost is obviously proportional to m for differencing operators based on Lagrange polynomials ([Berezin and Zhidkov 1965](#), pp. 212–214), and implementation of this family of differencing operators at different orders would result in a cost conforming to (2) with b independent of order m . Similarly compact differencing, interpolation, and integration schemes have a cost proportional to m ([Leslie and Purser 1992](#)) but with a value for b slightly different from the differencing operators above. Explicit advection schemes that involve cross terms such as that of [Leonard et al. \(1996\)](#) also have a cost approximately proportional to m (as can be seen from Fig. 13 of their manuscript).

Not all numerical schemes have computational cost proportional to m . For example, interpolation in a two-dimensional space using a Cartesian product of Lagrange interpolations would have a cost proportional to m^2 . But even in this instance alternative schemes exist ([Purser and Leslie 1991](#)) that have cost proportional to m . A high-order scheme that had a cost of m raised to a power greater than 1 can hardly be considered optimal and often more efficient alternatives can be found. The N -cycle time stepping proposed by [Lorenz \(1971\)](#) has a computational cost approximately independent of m but in this instance the high-order accuracy is only achieved every N th time step. Finally, it might be noted that although the number of operations might be proportional to m , the computational cost on vector computers can become more weakly dependent on m for straightforward differencing stencils. Thus, (2) is not universally applicable but it should be appropriate for many well-designed numerical schemes, and the following methodology can be easily adapted to cases where the computational cost is proportional to m^n where $n \neq 1$.

Many models have mixed-order numerics. Our analysis does not address mixed schemes. In the limit $\Delta \rightarrow 0$ it is clear that the lowest-order term must dominate the truncation error (providing the solution exercises all terms in the dynamics). Also, it might be argued that the time step need not be reduced at the same rate that the grid scale is reduced, which would lower the power D in (2). Certainly semi-Lagrangian methods (and some explicit advection schemes) are not limited by the CFL condition for stability. Nevertheless, for the truncation error to converge in a consistent manner it is necessary that the time step reduce proportional to the grid-scale refinement.

Consider an ocean model that has three spatial dimensions plus a temporal dimension and uses numerical methods with accuracy of order 2. If we reduce the grid scale by a factor of 2 and improve the order of accuracy of the numerical operators to order 4, then (1) shows that the error of such a model will be reduced by a factor of 16. On the other hand, (2) indicates that the computational cost will increase by a factor of 32. Now let us see how the same accuracy can be achieved without increasing the order of accuracy of the numerical operators. To reduce the error by a factor of 16 requires the grid scale be reduced by a factor of 4 in the case of second-order numerics. But such a reduction of grid scale requires the computational cost increase by a factor of 256, eight times the computational cost of the fourth-order scheme above!

Numerical computations are not only limited by computational speed but also by memory (RAM). It is noteworthy that the strategy above of increasing both the resolution and order by factors of 2 will result in the memory requirements being increased by a factor of 16 for inefficient temporal differencing schemes and 8 for optimal temporal differencing schemes ([Lorenz 1971](#)). On the other hand, obtaining the same accuracy by increasing the resolution by a factor of 4 (with order kept at 2) will result in memory requirements being increased by a factor of 32. Clearly, high-order numerics have the potential to substantially reduce memory requirements as well as computational cost.

A reviewer pointed out that the above computational cost advantage of increasing order relative to increasing grid resolution can be expressed more formally by considering two models, one at order m_1 and the other at order m_2 , that have the same truncation error ϵ . The two grid resolutions $[\Delta_1 = (\epsilon/a)^{1/m_1}, \Delta_2 = (\epsilon/a)^{1/m_2}]$ that give the same truncation error ϵ for two orders of accuracy (m_1, m_2) can be obtained from (1). The costs of the two models can be obtained by substituting

into (2) and the ratio of costs is

$$\frac{C_1}{C_2} = \frac{m_1}{m_2} \left(\frac{\epsilon}{a} \right)^{D[(1/m_2)-(1/m_1)]} \quad (3)$$

Thus, as $\epsilon \rightarrow 0$, the higher-order model will always be more efficient. Even nonoptimal schemes, where computational cost is proportional to m raised to some power n , have a cost ratio $(m_1/m_2)^n (\epsilon/a)^{D(1/m_2-1/m_1)}$, and again high-order numerics have the advantage for small ϵ .

In formulating (3) the proportionality constants a and b are assumed to be the same for both models. This means that, although the models are at different order, both models use the same numerical method (or methods belonging to families with the same values for a and b). This is consistent with our central purpose, which is to explore which order of numerical scheme is most effectively employed—not to argue the merits of one family of numerical schemes relative to another.

The above work is useful for comparing two similar models with different order numerics but gives little practical guidance to determine m in any absolute sense. Here we ask how high need the order of accuracy be to obtain the advantages of high-order differencing? For a given domain it is clear that as the grid spacing tends toward zero, then the error tends to zero, while the computational cost tends to infinity. This applies regardless of the order of differencing. Our question might be addressed by determining the relative rates of increase in computational cost and decrease in error as the grid is refined. (Note that m cannot be increased indefinitely without increasing the number of grid points.) An appropriate measure of the above relative rates of change can be obtained by considering the product of error and cost. In particular, we are interested in the behavior of this product as $\Delta \rightarrow 0$:

$$\lim_{\Delta \rightarrow 0} \epsilon C = \lim_{\Delta \rightarrow 0} abm \Delta^{(m-D)} = \begin{cases} \infty, & \text{if } m < D \\ abm, & \text{if } m = D \\ 0, & \text{if } m > D. \end{cases} \quad (4)$$

Clearly, if $m < D$, then grid refinement leads to computational cost growing faster than the truncation error is reduced. We might say that, if $m < D$, then error reduction by grid refinement is computationally inefficient. If, possibly for good reason, we are forced to adopt this strategy, then there is no substitute for computational effort and such models are computationally inefficient in the sense that grid refinement produces improved accuracy with a disproportionate increase in computational cost. When $m > D$, the truncation error can be reduced more quickly by grid refinement than the computational cost increases, and grid refinement is a computationally efficient strategy for error reduction. Note, in the limit $\Delta \rightarrow 0$, any value of m larger than D achieves the same limit, which indicates that the relative advantages diminish the more m is made larger than D . It would seem, therefore, appropriate to require $m > D$ with little advantage in making m much greater than D . A choice of $m = D + 1$ would seem practical for flows that exercise all terms in the equations of motion. In the instance that the numerical scheme being used has small values for a and b , then choosing $m = D$ might be argued to be adequate.

The asymptotic limit $\Delta \rightarrow 0$ is interesting but the behavior of ϵC as a function of m and Δ is also pertinent to considering model performance in instances when computational resources are limiting. Figure 1 plots $\ln(\epsilon C)$ as a function of Δ and m . At $\Delta = 1$ the error is not reduced by increasing the differencing order. It is easy to show that for centered differencing on an unstaggered grid $\Delta = 1$ corresponds to a grid spacing of half the smallest wavelength. On a staggered grid $\Delta = 1$ corresponds to a grid spacing equal to the smallest wavelength. Clearly, for $\Delta > 0.8$ the error diminishes too slowly with increasing m for high-order differencing to substantially reduce error compared to the increased computational cost. This behavior is obvious in the limit $\Delta \rightarrow 1$. But no numerical calculation can be accurate when Δ is near 1. As mentioned earlier, values of $\Delta \geq 1$ are pathological. Figure 1 shows that for $\Delta \leq 0.6$ the function ϵC indicates that high-order differencing becomes advantageous. The crossover resolution for high-order differencing appears to be Δ in the interval (0.6, 0.8). Figure 1 also confirms that our choice of $m \geq D + 1 = 4$ is appropriate not just for the asymptotic limit $\Delta \rightarrow 0$ but indeed for any $\Delta < 0.6$. Reasonable accuracy constraints require even more restrictive values of Δ so the asymptotic constraints in (4) are generally applicable.

In Fig. 1 the tight bunching of contours for small Δ and low order illustrates that high-resolution model calculations at second order are not cost effective. First-order calculations are well known not to be cost effective and are not shown in the figure.

Increasing an ocean model's order of accuracy is not an alternative to making Δ sufficiently small to resolve the physical processes being studied. Inasmuch as ocean flows have a wide range of scales, it follows that grid refinement will always be an important strategy. Certainly grid refinement is advantageous if energetic subgrid-scale processes cannot be

parameterized with confidence. In intermediate circumstances where high-order differencing and grid refinement are both useful strategies, then (4) suggests that m should be either D or $D + 1$ in order to reduce error in a computationally efficient manner.

3. Field singularities and the asymptotic assumption

The above arguments are of an asymptotic form and assume the error is dominated by the leading term in the error expansion. Counterarguments are concerned with the case when there is sufficient variability at the small scales (e.g., discontinuities like fronts) so that relatively little can be gained by increasing the order of accuracy compared to the immediate gains obtained (expensively) by increasing the resolution. Let us examine the extent to which singularities are likely to confound the advantages of high-order differencing for ocean models.

A scaling argument on the Navier–Stokes equations shows that the difference between velocity at a point \mathbf{x} and a velocity at a second point a distance l away from \mathbf{x} scales proportional to $l^{1/3}$ (Schertzer and Lovejoy 1989). The relative motion of pairs of particles has been the subject of considerable observational and theoretical interest in the context of eddy diffusion and the fractal properties of the ocean and atmosphere (Richardson 1926; Stommel 1949; Okubo 1971; Sanderson and Booth 1991). Generally the two-particle and patch eddy diffusivities are observed to vary as length scale raised to a power of about 4/3. On this basis the relative velocities would scale as separation distance raised to a power of 1/3 and differential kinematic properties (vorticity and divergence) would scale as separation distance to the power of $-2/3$. Kawai (1985) observed that vorticity and divergence had magnitudes consistent with the above scaling.

The above scaling of relative motion as a function of separation distance shows that we should expect the ocean to have flow-field singularities such that ever more intense flow gradients are observed as grid scale is reduced. Indeed, there is evidence that particle trajectories are fractal (Sanderson and Booth 1991) in which case differentiation only makes sense if we first apply some smoothing operator. The implication is that for a wide range of grid scales there will always be small-scale structure that has the potential to cause the flow to be insufficiently smooth for (1), (3), and (4) to apply.

4. Truncation error and unresolved fluctuations

Ocean flows have variability on a wide range of scales. This variability could be expressed by representing the flow as an infinite Fourier series. Figure 2 shows a conceptual diagram of the spectrum of some flow variable that has its variance distributed according to a power law. At a grid resolution Δ we will be able to resolve that portion of the spectrum with wavenumbers less than a cutoff wavenumber k_c . Variance at all wavenumbers higher than k_c must be omitted from the numerical model. A numerical differencing scheme can only approximate derivatives of the resolved portion of the flow field and will result in a truncation error ϵ_m that will be a function of the order of differencing m .

Let us increase the grid scale to δ ; then the model would only resolve that portion of the spectrum that is shaded in Fig. 2. Now there would be a new truncation error but there would be an additional error due to the unresolved fluctuations with wavenumbers less than k_c but not in the shaded region. Consider the case where the order of differencing on the coarse δ grid is twice that on the fine grid Δ . If $\delta = 2^{1/4}\Delta$, then this would correspond to an equivalent computational cost in the instance $D = 4$ (a numerical model with three spatial dimensions plus time). If the total error on the coarse grid is less than the truncation error on the fine grid, then high-order differencing is advantageous. The following analysis will formalize and apply the above discussion to determine the circumstances under which high-order differencing is advantageous.

Consider some quantity q that is differenced in the equations of motion. We might consider q to be $u^2/2$ or pressure p if we were considering terms such as field acceleration $u(\partial u)/(\partial x)$ or pressure gradient $\partial p/\partial x$ respectively. The quantity q might be represented as a Fourier series

$$q = \sum_{i=0}^{\infty} A_i \sin(ix + \phi_i), \quad (5)$$

where A_i is an amplitude, ϕ_i is a random phase uniformly distributed in $[0, 2\pi]$, and x varies over the domain $[0, 2\pi]$ thereby normalizing the smallest wavenumber. Here we will consider the case where A_i is proportional to some power of wavenumber:

$$A_i = \beta i^{-\alpha}. \quad (6)$$

The power is negative, indicating that there is more variability in large-scale flows than small-scale flows.

The spectrum of energy density might be $-5/3$ in the inertial subrange of three-dimensional turbulence. At larger scales associated with internal waves a spectral energy density with power law -2 might apply and at still larger scales associated with geophysical turbulence a power law of -3 might apply. Thus, if we were considering a finite-difference approximation to $\partial u/\partial x$, then q would be the u field and appropriate values of α would be $5/6$, 1 , and 1.5 respectively for three-dimensional turbulence, internal waves, and geophysical turbulence. (Larger values of α would result if the random phase assumption was relaxed). On the other hand, considering a finite-difference form to the field acceleration would mean setting q to scale like u^2 and appropriate values of α would be $5/3$, 2 , and 3 respectively for three-dimensional turbulence, internal waves, and geophysical turbulence.

Consider a numerical model that divides the domain $[0, 2\pi]$ into N equal intervals of length Δ . The model therefore resolves the following portion of the Fourier series for q :

$$q = \sum_{i=0}^{N/2} A_i \sin(ix + \phi_i), \quad (7)$$

and all higher wavenumbers must be omitted to avoid aliasing. The derivative of q can be obtained analytically as

$$q' = \frac{dq}{dx} = \sum_{i=1}^{N/2} A_i i \cos(ix + \phi_i). \quad (8)$$

Numerically differencing q as given by (7) (on a grid with spacing Δ) will result in a discrepancy from the analytic value due to truncation errors of the differencing method. For example, a second-order difference gives the following estimate for the derivative:

$$q'_{2,\Delta}(x) = \frac{1}{2\Delta} [q(x + \Delta) - q(x - \Delta)], \quad (9)$$

where q is specified by (7). The difference between q' and $q'_{2,\Delta}$ is the truncation error and is, therefore, directly calculated in sum and for individual wavenumbers in the truncated Fourier expansion. The truncation error at order m on the fine Δ grid is denoted by $\epsilon_{m,\Delta} = q'_{m,\Delta} - q'$.

Let us consider a second grid that is a factor of $2^{1/4} \approx 1.2$ more coarse than the first grid. The grid scale of this more coarse grid is denoted δ and $\delta = 2^{1/4}\Delta$. In a 4D model, increasing the grid scale by this factor will change the computational cost by a factor of 2 (if order of differencing stays the same). On this coarsened grid the Fourier series for q becomes

$$q = \sum_{i=0}^{N/2.4} A_i \sin(ix + \phi_i), \quad (10)$$

which has fewer terms than (7)—that is, we have omitted those terms between k_c and the shaded portion in Fig. 2. Numerically differencing at fourth-order on this coarse grid results in the same computational cost as differencing at second order on the fine grid. (More generally, differencing at order $2m$ on the coarse grid involves the same computational cost as order m on the fine grid.) A fourth-order differencing formula is

$$q'_{4,\delta}(x) = \frac{1}{6\Delta} [q(x - 2\Delta) - 8q(x - \Delta) + 8q(x + \Delta) - q(x + 2\Delta)], \quad (11)$$

where q is now given by (10). The error of the fourth-order differencing on the coarse grid can be obtained by subtracting $q'_{4,\delta}$ from q' in (8). More generally, we denote the error at order $2m$ on the coarse δ grid by $\epsilon_{2m,\delta} = q'_{2m,\delta} - q'$.

We expect $\epsilon_{2m,\delta}$ will differ from $\epsilon_{m,\Delta}$ in several ways. The numerical differencing error increases with increasing grid scale. Also, more high wavenumber terms must be omitted from the Fourier series as the grid is made more coarse, and this also causes error to increase with increasing grid scale. On the other hand, the higher the order of the differencing operator, the lower the truncation error. The critical question is whether increasing order of accuracy (thereby reducing truncation error) can compensate for increased truncation error and wavenumber omission errors as we coarsen the grid.

In [Table 1](#) we present the root-mean-square value of errors obtained by subtracting numerically determined differences from the analytic derivatives given by [\(8\)](#). An ensemble of 4000 independent Fourier series was used to determine each root-mean-square value. The numerical differencing operator acted on [\(7\)](#) for the fine grid Δ and [\(10\)](#) for the coarse grid 1.2Δ . The numerical differencing is done at these two resolutions and using differencing formulas with orders 1, 2, 3, 4, and 6. Values of the error were calculated for α set to values of 5/6, 2, 3, and 4.

Accuracy is achieved with less computational cost by increasing differencing order than by increasing grid resolution whenever α is greater than 2. When $\alpha = 2$, the advantages of increased order over increased resolution are neutral—except that there is still an advantage increasing order from 1 to 2. If α is less than 2 then the argument for high-order differencing generally fails, although an advantage can still be obtained by increasing the order from 1 to 2.

Above we have addressed errors associated with some commonly used differencing operators. It is not clear that $\alpha = 2$ will prove a critical number under all other numerical differencing schemes (e.g., compact schemes). Whatever numerical schemes a model is using, the methodology presented above could be applied to determine the relative advantages of high- and low-order versions of the scheme. Midpoint Lagrangian interpolation exhibits a critical value of $\alpha = 1.5$ for a choice between second-order and fourth-order calculations, for example.

Clearly, for pressure signals with sufficiently red spectra, the minimization of truncation error by increasing differencing order can compensate the increased errors due to truncation and additional unresolved fluctuations on a grid that is coarsened so computational cost is invariant. But the advantages become reduced as the order of differencing increases. To see this, consider the case $\alpha = 3$ in [Table 1](#) and consider the errors linked by lines of equal computational cost. Increasing order from first to second results in error reduction of $47.6 - 8.2 = 39.4$. First-order differencing is generally not favored—for good reason. Going from second- to fourth-order reduces error by $6.08 - 4.37 = 1.71$, which is a 28% error reduction. Clearly, substantial gains might be expected by improving a second-order accurate model to be fourth-order accurate. Fourth-order numerical calculations do not result in significant coding difficulties, especially if a defect correction can be applied to an existing second-order calculation. Increasing order from third to sixth reduces error by $4.03 - 3.67 = 0.36$, which is only a 9% error reduction. This is consistent with [\(4\)](#) and indicates achieving orders substantially larger than D may not be worth the additional coding effort.

It is notable that on a vector processor a fourth-order operator such as [\(11\)](#) has a computational cost similar to a second-order operator [\(9\)](#). Comparing columns in [Table 1](#) it is clear that in such a circumstance high-order differencing will always yield an advantage and that advantage becomes more substantial as α increases. In terms of [\(1\)](#) we might infer that Δ (or similarly ϵ/a) becomes ever smaller than unity as α is increased.

As mentioned earlier, different terms in the equations of motion might have different values of α for a given flow. If a geophysical flow has a spectrum of kinetic energy with a -3 power law then α would be 3 for the field accelerations but only $3/2$ for terms in the continuity equation $\nabla \cdot \mathbf{u}$. In such a circumstance the field accelerations should be computed using high-order differencing, but low-order differencing would suffice for other terms. In the case of a three-dimensional energy cascade in the inertial subrange the spectrum has a slope of $-5/3$ and high-order differencing is unlikely to be helpful for any terms in the equations of motion (except for circumstances where computational cost increases more slowly than m or when the calculation is memory limited).

It is notable that high-order schemes can lead to undershoots and overshoots (i.e., nonphysical loss of monotonicity) when differencing fields that have discontinuities. A fourth-order compact differencing scheme, for example, is very sensitive to 2Δ signals even though it is much more accurate than [\(9\)](#) or [\(11\)](#) when differentiating a more smoothly varying function. The ocean is full of inconvenient boundaries and abrupt bathymetric features that have the potential to cause such discontinuities. The inertial subrange of a three-dimensional turbulent flow generates such discontinuities. Flow discontinuities are not expected to be space filling because of the fractal properties of turbulence discussed earlier. Thus, flows might be differenced at high order where they are smooth and limiters applied to avoid spurious oscillations at discontinuities ([Leonard et al. 1995](#)). In this manner, high-order operators might yet yield an advantage even when $\alpha < 2$. [Leonard et al. \(1996\)](#) demonstrates the practical implementation of high-order advection schemes (with limiters) that have advantages even for highly deformational flows and discontinuous fields.

In reality, ocean models are used to study all sorts of flows for many purposes. A forecasting model, for example, might be initialized using a dataset that has low spatial resolution. Clearly, the solution will not contain much energy at high wavenumbers (at least for the period it is likely to be useful for providing a meaningful forecast). In such circumstances we expect high-order differencing to yield substantial advantages and this has already been demonstrated for numerical weather forecasting ([Purser and Leslie 1988](#)).

In the following work we will analyze solutions obtained by applying several ocean models to a range of oceanic problems in order to determine the extent to which these model applications may or may not benefit from high-order differencing.

5. The applicability of high-order differencing to some ocean simulations

In [section 4](#) we have always assumed a power-law relationship that applies to all wavenumbers (or equivalently frequencies). If the energy in the small wavenumbers is somewhat less than indicated by the power law, then this turns out to be of no consequence to the above discussion because the error in numerically differencing these small wavenumbers is negligible compared to the higher wavenumbers. It is the slope of the power spectral density function near the cutoff wavenumber that is most important. At this stage it is helpful to visualize signals q that can be represented as a Fourier series [\(7\)](#) with $N = 120$ and A_i given by

$$A_i = \frac{\beta}{1 + (i/5)^\alpha}, \quad (12)$$

which asymptotes to the same form as [\(6\)](#). [Figure 3](#) shows A_i plotted against i on a log-log scale for values of $\alpha = 1, 2, 3, 4$. [Equation \(12\)](#) is perhaps more consistent with natural signals than [\(6\)](#). Signals obtained from [\(7\)](#) and [\(12\)](#) are plotted in [Fig. 4](#) with successive signals vertically offset for clarity. A common set of random phases ϕ_i was used for each signal plotted in [Fig. 4](#). The signal corresponding to $\alpha = 1$ is probably better treated using low-order numerics. On the other hand, the smoother signals corresponding to α greater than 2 are best treated using high-order numerics.

Providing the power spectral energy density falls off sufficiently quickly with increasing wavenumber (or frequency), then high-order differencing will be advantageous. Power spectra of output from several numerical simulations will now be considered to determine if high-order differencing would benefit these calculations.

England and Garcon (1994) ran a 1.6° resolution global ocean circulation model. Output from the Southern Ocean (bounded by latitudes 77° to 60°S) exhibits high wavenumber variability. [Figure 5](#) shows that the spectral densities and cross-spectral density of the velocity components all approximately conform to -4 power laws at high wavenumbers. Field accelerations scale as the derivative of kinetic energy, so $\alpha = 4$ and the advantages of high-order calculation of the field acceleration would be substantial. The power spectrum of temperature T indicates a -4 power law except for grid-scale instabilities at these high latitudes that are associated with high Courant numbers. Clearly, this model would also benefit from a high-order advection scheme that is not time step limited. [Leonard \(1994\)](#) discusses the relationship between Courant number and stability for various numerical schemes.

I have done a 100-yr idealized simulation of the East Australian Current using the DieCAST primitive equation model run at $1/4^\circ$ resolution. The model domain extended over latitudes -46° to -18° and from the east coast of Australia to New Zealand. The western boundary was landlocked, and the southern and eastern boundaries were open. A geostrophic inflowing jet of warm water was impressed on the northern boundary at the Australian shelf break with a transport of 13 Sv. Advective transport conditions were used at the open boundaries with a weak relaxation to climatology. The resulting fields at open boundaries were averaged as the model was run and used to update the boundary climatology. After year 6 the boundary climatology was fixed. The eddy viscosity was set to $500 \text{ m}^2 \text{ s}^{-1}$ near the open boundaries and reduced by two orders of magnitude away from open boundaries.

A complex and ever changing eddy field is observed where the East Australian Current separates from the coast, and an example is shown in [Fig. 6](#). Monthly snapshots of model fields over the last 60 years of the simulation will be used for the analysis below. Power spectra and the cross-spectrum for the two components of velocity ([Fig. 7](#)) clearly indicate the advantage to be obtained using high-order schemes for the field accelerations. The surface pressure signal has a power spectral density that falls off faster than -4 except for the highest wavenumbers, which are contaminated by twice-grid-scale noise. The temperature signal is even more strongly contaminated by twice-grid-scale noise. Except for the twice-grid-scale contamination the Fourier transform of surface pressure would correspond to $\alpha \approx 3$. DieCAST uses a fourth-order scheme for advection and a second-order scheme for pressure gradients. For the simulation reported here, it would seem some advantage could be obtained by going to higher order when calculating pressure gradients (although the gains of high-order determination of field accelerations are greater).

The above work pertains to hydrostatic dynamics first for large-scale climatological flows and second for eddy fields associated with major ocean currents. Nonhydrostatic convection results in much smaller scale structure and provides a quite different context in which to test the applicability of high-order differencing. A two-dimensional (x - z) nonhydrostatic, rigid-lid, Boussinesq model has been constructed using semi-Lagrangian methods. The model is second-order in time, eighth-order for advective terms, and fourth-order for other spatial derivatives. Observed temperature profiles in a billabong (small lake about 2 m deep by 100 m wide) have been simulated by forcing the model with observed nighttime heat fluxes. The model was initialized with the observed temperature profile, which had varied from a surface temperature of 26.5°C to a temperature of about 24.5°C at depth. The grid scale is 0.054 m with adaptive time stepping. [Figure 8](#) shows a snapshot of temperature contours and the velocity field 3.5 hours after the onset of surface cooling. Let us analyze fields from the

convecting surface boundary layer where the highest wavenumber features are most evident.

At high wavenumbers the power spectral densities of u and T conform to power laws of about -4.5 as indicated by the plots in [Fig. 9](#). The cross-spectral density between u and w has an even steeper slope (approximately -5.3). It follows that field acceleration and advection should be treated using high-order numerical schemes. The lower right plot in [Fig. 9](#) shows the power spectral density of the pressure field conforms to a power law of about -5.3 if we ignore twice-grid-scale energy, which has doubtful physical significance. For pressure $\alpha \approx 2.6$, and we might conclude that high-order differencing is advantageous for determining the pressure gradient.

The error resulting from order m numerical differencing of a function q can generally be written

$$\epsilon = \sum_{i=0}^{\infty} a_{m+i} \Delta^{m+i} q^{(m+i+1)}, \quad (13)$$

where $q^{(k)}$ denotes the k th derivative and a_k is some constant such that $a_{k+1} < a_k$. For example, in the case of second-order centered numerical differencing

$$q'(x) = \frac{q(x + \Delta) - q(x - \Delta)}{2\Delta} - \frac{1}{2} \sum_{n=1}^{\infty} \frac{\Delta^{2n}}{(2n + 1)!} q^{(2n+1)}. \quad (14)$$

Clearly, the series

$$\sum_{n=1}^{\infty} \frac{1}{(2n + 1)!}$$

converges rapidly. It follows that if $q^{(2n+1)}$ does not increase significantly with increasing n , then the error is dominated by the first term in the residual series.

[Equation \(1\)](#) applies in the limit that error ϵ is dominated by the first term in the above series. If [\(1\)](#) applies (and given $\epsilon/a < 1$), then [\(3\)](#) and [\(4\)](#) can guide a decision as to the advantages of high-order differencing versus low-order differencing. Directly testing the applicability of [\(1\)](#) is difficult, so the alternative strategy of [section 4](#) was developed. Nevertheless, it should be possible to infer some information about the applicability of [\(1\)](#) in a direct way.

A direct test of [\(1\)](#) requires evaluation of the derivatives of q in order to determine whether or not the asymptotic limit applies. An m th order ocean model will give solutions from which all the derivatives $q^{(n)}$ up to $n = m$ might be estimated. This suggests the following strategy for examining the applicability of [\(1\)](#). Using high-order numerics ($m = 6$) a nontrivial problem of oceanographic significance will be solved. We can then estimate the relative values of the first few residual terms in [\(13\)](#) that might result from a second-order ($m = 2$) model. Thus, we use a high-order scheme to directly calculate the first few terms in the residual series of a low-order scheme.

[McCalpin \(1995\)](#) used a $1\frac{1}{2}$ -layer quasigeostrophic model to study the statistics of a double gyre on a Northern Hemisphere beta plane for an ocean basin that spanned 2800 km in the y direction (latitude) and 3600 km in the x direction (longitude) and had a 20-km grid. The above model was forced by a wind stress that varied sinusoidally with y (normalized to the range $[0, 1]$), had an amplitude of $\tau_0 = 0.5 \text{ m}^2 \text{ s}^{-2}$:

$$\tau_x = -\tau_0 \cos(2\pi y)[1 - 4\gamma(y - 1/2)] \quad (15)$$

in which γ is an asymmetry factor. Below we use the same forcing for our own reduced-gravity model.

Over the scale of an ocean basin there are substantial differences in the temperature of the surface layer. Including these temperature differences leads to the following reduced-gravity equations:

$$\frac{dh}{dt} + h\nabla \cdot \mathbf{u} = 0, \quad (17)$$

where d/dt indicates the total derivative, h is the surface-layer thickness, r_i is an interfacial drag coefficient, and f is the Coriolis parameter. The reduced gravity g' is determined from the local densities ρ_s and ρ_l in the surface and lower layers respectively:



$$g' = g \frac{\rho_l - \rho_s}{\rho_l}. \quad (18)$$


The density is determined from temperature T and salinity S using the [UNESCO \(1981\)](#) equation of state. Temperature and salinity satisfy the advection equations ($dT/dx = 0$, $dS/dx = 0$), and temperature is restored to a uniform north–south gradient such that a column 100 m deep e -folds over a 30-day period.

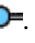


The above reduced-gravity equations were solved following the semi-Lagrangian model of [Purser and Leslie \(1988\)](#) except that the improved [Purser and Leslie \(1991\)](#) high-order cascade interpolation method was used and a fast algorithm ([McGregor 1993](#)) was used to calculate back displacements. The numerical scheme is second-order in time, and we ran it at sixth order for spatial derivatives except field accelerations and advective terms were calculated at eighth order.

The major difference between our system and that of [McCalpin \(1995\)](#) is the inclusion of baroclinicity effects associated with horizontal temperature gradients. Other differences were the exclusion of horizontal eddy viscosity and a modification to the interfacial drag. Horizontal eddy viscosity is not included since the physical basis for horizontal eddy viscosity is doubtful ([Harrison 1978](#)). The interfacial friction was set at 10^{-7} s^{-1} consistent with McCalpin in deep water, but was set to $1.5 \times 10^{-6} \text{ s}^{-1}$ at boundary points and $5 \times 10^{-7} \text{ s}^{-1}$ one grid in from the boundary in order to crudely parameterize the increased bottom friction associated with the shelf break.

Following [McCalpin \(1995\)](#) a 140 (y) by 180 (x) grid was used with a time step of 7200 s but the grid scale was increased slightly to 22 km. The surface temperature field initially varied linearly from 25°C in the south to 15°C at the northern boundary. Subsequently the surface temperature was restored to this initial field. Salinity was set at 34 psu throughout, and the lower-layer temperature was set at 2°C. Initially the interfacial depth was set so as to balance the north–south temperature field without any motion and with a mean surface-layer depth of 600 m (consistent with McCalpin). The model was then forced with a steady wind stress [\(15\)](#) with asymmetry factor $\gamma = 0.05$.

The currents showed continuous variability particularly surrounding the separation of the western boundary currents. [Figure 10](#)  shows the interfacial thickness (relative to its initial equilibrium value) after 20 years and a more detailed plot of the velocity field near the separation point. An ever-changing spatially variable flow is evident near the separation point (see <http://www.maths.unsw.EDU.AU/bxs/Tmovie.gif> for a movie of temperature). The lower right panel of [Fig. 11](#)  shows that contours of temperature also exhibit sharp gradients associated with separation of the western boundary current.

[Figure 11](#)  shows the power spectral density of fields obtained from the boxed area in the lower right plot. Clearly, the spectra fall off sufficiently sharply for high-order differencing to be advantageous. This model is a gross simplification of a full 3D ocean model and the complex geometries of real ocean basins. It is not surprising, therefore, that such idealized models seem to have less high wavenumber energy and are therefore most amenable to high-order differencing.

The absolute value of $\Delta^n h^{(n)}$ summed over all points in the model domain was obtained for $n = 1, 2, \dots, 8$ and plotted in [Fig. 12a](#) . [Figures 12b–d](#)  shows equivalent plots for temperature and velocity field. As n is increased from 1 to 6, we observe $\Delta^n h^{(n)}$ generally become smaller. A small rise is noted as n increases from 6 to 8, which is consistent with the model having spatial differencing of mixed sixth and eighth orders. The tendency for slight positive slopes at large n is a consequence of the quantities being calculated near the formal limits of the the models order of accuracy. Ultimately, machine round off errors will also limit how high m and n can be made. [Figure 13](#)  shows the maximum values of $\Delta^n h^{(n)}$, $\Delta^n T^{(n)}$, $\Delta^n u^{(n)}$, and $\Delta^n v^{(n)}$ drop off less quickly over the resolved range of n , but still there can be little doubt that the first term dominates the residual series in [\(13\)](#). The evidence suggests that the series in [\(13\)](#) converges very rapidly and [\(1\)](#) is applicable. This indicates in a direct manner that the results developed in [section 2](#) are applicable for this particular model.

It is noteworthy that sharp fronts consist of spectral components of all scales. High wavenumber components (e.g., $2 - \Delta x$) are not accurately treated regardless of the differencing order. The advantage of the high-order differencing operators is that slightly lower wavenumber constituents of the front are more accurately represented. Unfortunately, the simple-minded application of high-order operators to regions with rapidly changing gradients can result in unphysical oscillations. [Leonard et al. \(1995\)](#) illustrates how limiters can be applied to obviate this problem rather than reverting to dissipative low-order

schemes.

Many of the premier models used by the oceanographic community are only first- or second-order accurate ([Haidvogel and Beckmann 1997](#)). Perhaps the reason why the low-order models perform “well enough” is that the ocean currents they model are mostly two-dimensional (varying slowly with respect to time and having little vertical motion). In the limit when resolution is increased so that ocean models start to resolve smaller scale physical processes, the time and vertical dimensions will no longer play such a minor role and the limitations of these low-order models should become apparent.

[Dietrich et al. \(1990\)](#) used grid convergence studies to demonstrate that “more accurate treatments of the Coriolis and pressure gradient terms, which generally dominate geophysical flows, provide converged solutions with lower resolution and, correspondingly less computation than required by the lower-order interpolation treatments of classical approaches, including the treatment used by the Bryan–Semtner–Cox model ([Semtner and Chervin 1988](#)).” The DieCAST model ([Dietrich et al. 1990](#)) uses fourth-order numerics for field accelerations although the pressure calculation is still done at second-order accuracy. The Dietrich results are consistent with the present analysis and indicate that the benefits of increased resolution are best achieved using high-order numerical schemes.

6. Conclusions

In a smooth flow where the grid scale is sufficiently small to resolve all wavenumber components, then it is always computationally more efficient to reduce truncation error by increasing differencing order than by reducing grid scale. Even when the model cannot resolve all scales of variability, high-order differencing will be beneficial providing the high wavenumber variability is not too energetic. To quantify what too energetic means we consider differencing a quantity that can be represented by a Fourier series with high wavenumber amplitudes diminishing according to a $-\alpha$ power law. Providing $\alpha > 2$ we find high-order differencing will increase accuracy with less computational cost than grid refinement. To resolve smaller-scale flow features it is, of course, still necessary to refine the grid. Increasing the order of the numerical differencing cannot compensate for a failure to resolve an important physical scale (such as the internal Rossby radius).

Successive increments of the order of differencing yield diminishing returns. As the grid is refined, we can consider the rate of increase of computational cost and the rate of decrease of error and how this depends upon the order m of differencing and the space–time dimension D of the problem being solved. It turns out that, if $m < D$, the computational cost grows more rapidly than the error decreases whereas, if $m > D$, the computational cost grows slowly compared to the rate at which error is reduced. Hence, when the flow has $\alpha > 2$, then accuracy is best obtained by grid refinement using differencing of order $D + 1$. Differencing of order D would also be satisfactory in that grid refinement would cause computational cost to increase at the same rate error is reduced. Differencing of order less than D should definitely not be used.

Flows with energetic high wavenumbers $\alpha < 2$ might best be modeled using lower-order numerics, in which case grid refinement is the only strategy for error reduction. In such circumstance accuracy is only achievable at a disproportionate computational cost for multidimensional ocean modeling. High-order differencing still yields more accurate solutions at a given grid scale when $\alpha < 2$. Computational memory can limit the resolution of an ocean model. High-order schemes have the advantage of reducing truncation error with the minimal requirement for further random access memory. Thus, even when $\alpha < 2$, high-order methods might be useful. Indeed, natural flows with $\alpha < 2$ might still have substantial portions of their domain that are relatively smooth, and in such circumstances high-order methods employing limiters have potential advantages relative to low-order schemes.

The power spectral densities of output from several numerical models were examined. In all cases it seemed that differencing associated with advective terms would benefit substantially from the use of high-order schemes since values of α were invariably larger than 4. Other terms usually had smaller values of α but not so small that high-order differencing could not be justified.

Ocean models with high-order numerics can be used to directly examine whether or not the numerical error is dominated by the first term in the truncation series for models using low-order numerics. The two-gyre problem was studied using an idealized model of a rectangular ocean domain. Fields obtained from the calculation were smooth $\alpha > 4$. Calculation of first to eighth derivatives indicated that the first terms would indeed dominated the truncation series, indicating that (1) is applicable. The resulting scale analysis further suggests that high-order numerics are advantageous for this calculation. Third- or fourth-order would suffice, given that this calculation has one temporal dimension and only two spatial dimensions.

In view of the results obtained, it would appear that there are many circumstances in which ocean models should use fourth- or higher-order numerics for at least some terms in the equations of motion. In particular, for forecasting purposes models are often initialized with relatively sparse datasets, and in such circumstances it is the accuracy with which lower wavenumber information can be extrapolated forward that determines the forecast usefulness. Clearly, forecasting models

might usefully employ high-order numerical schemes. There is no unique answer to the issue of order versus resolution that is applicable to all flows, but this manuscript has presented a method by which the relative merits can be determined as a function of the flow properties being modeled.

Acknowledgments

I thank two anonymous reviewers who greatly improved the interpretation of the scaling analysis. Correspondence with R. J. Purser stimulated me to pursue this work and helped formulate some of my preliminary ideas.

REFERENCES

- Bender, L. C., 1996: Modification of the physics and numerics in a third-generation ocean wave model. *J. Atmos. Oceanic Technol.*, **13**, 726–750..
- Berezin, I. S., and N. P. Zhidkov, 1965: *Computing Methods*. Vol. 1. Pergamon Press, 464 pp..
- Dietrich, D. E., P. J. Roache, and M. G. Marietta, 1990: Convergence studies with the Sandia Ocean Modeling System. *Int. J. Numer. Methods Fluids*, **11**, 127–150..
- Haidvogel, D. B., and A. Beckmann, 1997: Numerical modeling of the coastal ocean. *The Sea*, **10**, 457–482..
- , E. Curchitser, M. Iskandarani, R. Hughes, and M. Taylor, 1997: Global modeling of the ocean and atmosphere using the spectral element method. *Atmos.–Ocean*, **XXXV** (1), 505–531..
- Harrison, D. E., 1978: On the diffusion parameterization of mesoscale eddy effects from a numerical ocean experiment. *J. Phys. Oceanogr.*, **8**, 913–918..
- Iskandarani, M., D. B. Haidvogel, and J. P. Boyd, 1994: A staggered spectral finite element model for the shallow water equations. *Int. J. Numer. Methods Fluids*, **20**, 393–414..
- Kawai, H., 1985: Scale dependence of divergence and vorticity of near-surface flows in the sea. Part 2, Results and interpretation. *J. Oceanogr. Soc. Japan*, **41**, 167–175..
- Leonard, B. P., 1994: Note on the von Neumann stability of explicit one-dimensional advection schemes. *Comput. Methods Appl. Mech. Eng.*, **118**, 29–46..
- , A. P. Lock, and M. K. MacVean, 1995: The NIRVANA scheme applied to one-dimensional advection. *Int. J. Numer. Methods Heat Fluid Flow*, **5**, 341–377..
- , —, and —, 1996: Conservative explicit unrestricted time-step multidimensional constancy-preserving advection schemes. *Mon. Wea. Rev.*, **124**, 2588–2606.. [Find this article online](#)
- Leslie, L. M., and R. J. Purser, 1992: A comparative study of the performance of various vertical discretization schemes. *Meteor. Atmos. Phys.*, **50**, 61–73..
- Lorenz, E. N., 1971: An N -cycle time-differencing scheme for stepwise numerical integration. *Mon. Wea. Rev.*, **99**, 644–648.. [Find this article online](#)
- Mahadevan, A., J. Oliger, and R. Street, 1996: A nonhydrostatic mesoscale ocean model. Part II: Numerical implementation. *J. Phys. Oceanogr.*, **26**, 1881–1900..
- McCalpin, J. D., 1994: Comparison of second-order and fourth-order gradient algorithms in a σ -coordinate ocean model. *Int. J. Numer. Methods Fluids*, **18**, 361–383..
- , 1995: The statistics and sensitivity of a double-gyre model: The reduced-gravity, quasigeostrophic case. *J. Phys. Oceanogr.*, **25**, 806–824..
- McGregor, J. L., 1993: Economical determination of departure points for semi-Lagrangian models. *Mon. Wea. Rev.*, **121**, 221–230.. [Find this article online](#)
- Okubo, A., 1971: Oceanic diffusion diagrams. *Deep-Sea Res.*, **18**, 789–802..
- Purser, R. J., and L. M. Leslie, 1988: A semi-implicit, semi-Lagrangian finite-difference scheme using high-order spatial differencing on a

—, and —, 1991: An efficient interpolation procedure for high-order three-dimensional semi-Lagrangian models. *Mon. Wea. Rev.*, **119**, 2492–2498.. [Find this article online](#)

Richardson, L. F., 1926: Atmospheric diffusion shown on a distance-neighbour graph. *Proc. Roy. Soc. London, Ser. A*, **110**, 709–737..

Sanderson, B. G., and D. A. Booth, 1991: The fractal dimension of relative Lagrangian motion. *Tellus*, **43A**, 334–349..

Schertzer, D., and S. Lovejoy, 1989: Generalized scale invariance and multiplicative processes for the atmosphere. *Pure Appl. Geophys.*, **130** (1), 57–81..

Semtner, A. J., and R. M. Chervin, 1988: A simulation of the global ocean circulation with resolved eddies. *J. Geophys. Res.*, **93**, 15 502–15 522..

Stommel, H., 1949: Horizontal diffusion due to oceanic turbulence. *J. Mar. Res.*, **8**, 199–225..

UNESCO, 1981: Tenth report on the joint panel on oceanographic tables and standards. UNESCO Technical Papers in Marine Science 36..

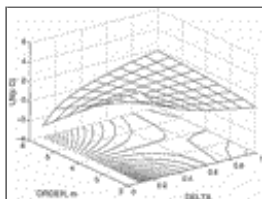
Tables

Table 1. Root-mean-square error as a function of, α , differencing order, and grid scale. Lines link error values where resolution and order would combine to cause equal computational cost in the context of a model with three space dimensions and the time dimension.

α	Order	10^3 error at Δ	10^3 error at 1.2Δ
5/6	1	5018	5241
5/6	2	3484	4118
5/6	3	3470	4114
5/6	4	2943	3771
5/6	6	2672	3610
2	1	184	209
2	2	94	118
2	3	87	111
2	4	69	95
2	6	59	87
3	1	47.6	57.0
3	2	6.08	8.24
3	3	4.03	5.74
3	4	2.92	4.37
3	6	2.31	3.67
4	1	1.205	1.446
4	2	0.0513	0.0737
4	3	0.00909	0.0144
4	4	0.00455	0.00752
4	6	0.00303	0.000527

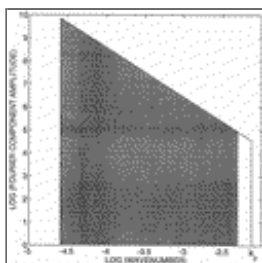
[Click on thumbnail for full-sized image.](#)

Figures



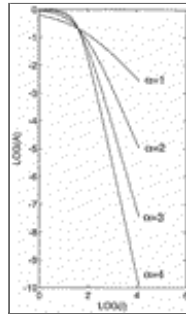
[Click on thumbnail for full-sized image.](#)

Fig. 1. The natural logarithm of C plotted as a function of Δ and order m . The plot shows a three-dimensional mesh with contours projected onto the base.



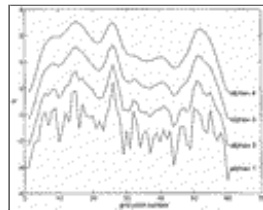
[Click on thumbnail for full-sized image.](#)

Fig. 2. Conceptual diagram of the power spectral density of a flow field. A low-order model resolves wavenumbers up to k_c . A high-order model with the same computational cost resolves wavenumbers in the shaded area. The high-order model does more accurate differencing of resolved wavenumbers than the low-order model but omits more wavenumbers.



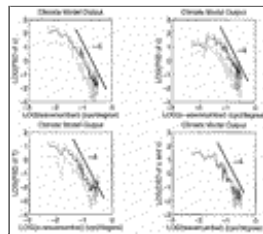
[Click on thumbnail for full-sized image.](#)

Fig. 3. Fourier amplitude coefficients A_i (12) plotted against wavenumber i on a log-log scale for values of α of 1, 2, 3, and 4.



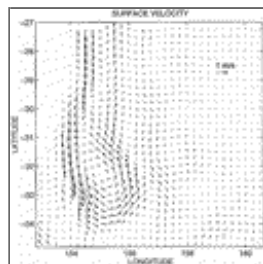
[Click on thumbnail for full-sized image.](#)

Fig. 4. Visualization of fields with the Fourier amplitude coefficients A_i plotted in Fig. 3. The fields are vertically offset and correspond to α of 1, 2, 3, and 4 as we progress from the bottom line to the top line. Fields become smoother as α is increased.



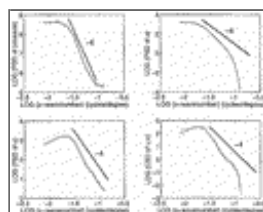
[Click on thumbnail for full-sized image.](#)

Fig. 5. Power spectral densities (PSD) and cross-spectral density (CSD) of u , v velocity components and temperature T in the Southern Ocean from a climatological ocean model integration by England and Garcon (1994).



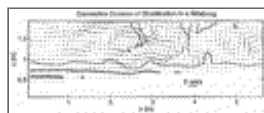
[Click on thumbnail for full-sized image.](#)

Fig. 6. Representative snapshot of the surface velocity field in an idealized simulation of the East Australian Current using the DieCAST ocean model run at $1/4^\circ$ resolution with 20 vertical levels.



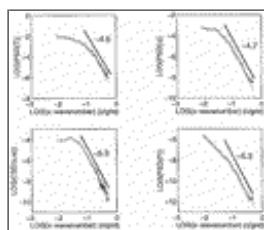
[Click on thumbnail for full-sized image.](#)

Fig. 7. Power spectral densities of surface pressure and velocity components obtained from an idealized simulation of the East Australian Current. Dotted lines indicate the 95% confidence interval. The cross spectral density between u and v is also shown for its relevance to the field acceleration term $u(\partial v)/(\partial x)$.



Click on thumbnail for full-sized image.

Fig. 8. Velocity and temperature fields for a small segment of a convecting billabong 3.5 hours after the onset of nighttime cooling. The segment plotted is a small part of the model domain and is located about three-quarters of the way across the 100-m-wide billabong. Temperature contours are 24.5°, 25°, and 25.5°C progressing from the thick to thin contour lines. Velocity vectors are shown at every second model grid point.



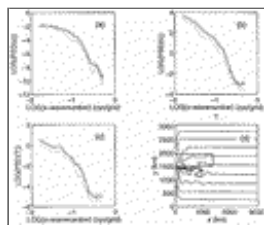
Click on thumbnail for full-sized image.

Fig. 9. Power spectral densities of temperature T , the horizontal velocity component u , and the nonhydrostatic pressure P from a convecting layer in a billabong. Also shown is the cross-spectral density between u and w velocity components. The dotted lines indicate 95% confidence intervals.



Click on thumbnail for full-sized image.

Fig. 10. This reduced-gravity model is initially at rest with a uniform north–south temperature gradient being balanced by a north–south pressure gradient. The model is forced from equilibrium by an asymmetric wind stress. The top plot shows the deviation of surface-layer thickness from its rest state value. Dashed contours are at –20 m intervals and solid contours are at 20-m intervals. The plot omits the 40 most eastern points in the model domain. The lower plot shows a segment of the velocity field in the vicinity of the separating western boundary current.



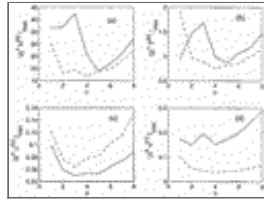
Click on thumbnail for full-sized image.

Fig. 11. The lower right plot shows temperature contours at 1°C intervals for the region plotted in [Fig. 10](#). The temperature ranges from 25°C on the southern boundary to 15°C on the northern boundary. Power spectral densities for u , h , and T fields within the boxed area are presented.



Click on thumbnail for full-sized image.

Fig. 12. Absolute value of $\Delta^n q^{(n)}$ summed over all points in the model domain plotted against n : (a) derivatives of the surface-layer thickness, (b) derivatives of surface-layer temperature, (c) derivatives of u velocity component, and (d) derivatives of v velocity component. The u , v , T , and h fields were calculated using a model with mixed sixth- and eighth-order spatial differencing.



Click on thumbnail for full-sized image.

Fig. 13. Maximum absolute value of $\Delta^n q^{(n)}$ plotted against n : (a) derivatives of the surface-layer thickness, (b) derivatives of surface-layer temperature, (c) derivatives of u velocity component, and (d) derivatives of v velocity component.

Corresponding author address: Dr. Brian Sanderson, School of Mathematics, UNSW, New South Wales 2052, Australia.

E-mail: bxs@maths.unsw.edu.au

top ▲



© 2008 American Meteorological Society [Privacy Policy and Disclaimer](#)
Headquarters: 45 Beacon Street Boston, MA 02108-3693
DC Office: 1120 G Street, NW, Suite 800 Washington DC, 20005-3826
amsinfo@ametsoc.org Phone: 617-227-2425 Fax: 617-742-8718
[Allen Press, Inc.](#) assists in the online publication of AMS journals.